John R. Jensen
Michael E. Hodgson
Department of Geography
University of South Carolina
Columbia, SC 29208

Remote Sensing Brightness Maps

Principles and algorithms are presented which enable pseudo continuous-tone brightness maps to be produced using plotters.

Abstract: *Remote sensing brightness maps are produced for almost every education or research remote sensing project which makes use of digital data. The production of such maps is dependent on (1) the type of output device available, and (2) the type of algorithm(s) or logic applied to the data. Brightness maps produced on high resolution CRTs or film writers, line printers, and line plotters are discussed. The unfortunate necessity to generalize the digital remote sensing data is reviewed in the context of density sliced maps produced on the line printer. Crossed-line symbolization produced on an electrostatic printer-plotter, which closely approximates the ungeneralized continuous-tone brightness maps produced on more expensive output devices, is discussed. Aspects of perceptual scaling, contrast stretch enhancement, and the degree of edge-growth expected during reproduction are reviewed.*

Introduction

Black-and-white aerial photography exhibits a continuous-tone range of gray values. The photointerpretation of such imagery is possible because human beings process continuous-tone images throughout their daily existence. But what of the plethora of digital remotely sensed data which is available from sensor systems such as Landsat? How does an interpreter convert the digital number (DN) brightness values stored on a computer compatible tape (CCT) into an image which begins to approximate the continuous-tone photographs he or she is used to interpreting? The answer is the creation of a brightness map, also commonly referred to as a gray-scale map.† Almost every digital image processing system designed for remote sensing education or research purposes has the capability to produce brightness maps (Carter *et al.*, 1977; Jensen *et al.*, 1979). The quality of the remote sensing brightness maps is dependent on (1) the type of output device and (2) the type of algorithm(s) or logic applied to the data. This paper describes remote sensing brightness maps produced by various output devices. It then identifies algorithms for use on an electrostatic printer-plotter which produce continuous-tone output very similar in appearance to that produced by more expensive output devices.

Data Format

Brightness values obtained from the Landsat multispectral scanner (MSS) system are used in this

† There are two fundamental types of brightness maps; the remote sensing brightness map and the hill shading brightness or reflectance map. There are important differences between the two types of maps. First, the data bases are different. The shades of gray plotted on a remote sensing brightness map are the result of analyzing wavelength dependent radiant flux reflected or emitted by Earth surface materials and recorded by a remote sensing device. Thus, the spectral characteristics of the land cover (e.g., soil, vegetation, water) are very important. The hill shading reflectance map is simply a plot of apparent brightness versus two variables: the slope of the Earth's surface in the west to east and south to north direction (Yoeli, 1966; Horn, 1979). The digital terrain model represents the fundamental data base for hill-shading maps, with the reflectance characteristics of surface cover being insignificant. The second major difference is purpose. The remote sensing brightness map provides a two-dimensional impression of terrain reflectance or emittance characteristics and shape. Conversely, the hill shading map is designed to provide a three-dimensional impression of terrain shape and especially relief (Brassel, 1974; Horn, 1981). The cartographic data structure for both types of brightness maps is usually the matrix, with the picture element (pixel) being the minimum mapping unit.

Photogrammetric Engineering and Remote Sensing,
Vol. 49, No. 1, January 1983, pp. 93-102.

0099-1112/83/4901-93$02.25/0

paper. The brightness values for Landsat bands 4, 5, and 6 are recorded on CCTs using a seven-bit scale (0 to 127) while band 7 is recorded on a six-bit scale (0 to 63). Many digital image processing systems initially rescale the six- and seven-bit data to eight bits (i.e., values from 0 to 255). There are a variety of algorithms which can perform the rescaling (Castleman, 1979). One commonly used method is to multiply the original values by two (for bands 4, 5, and 6) or four (for band 7) to produce an eight-bit range (Sabins, 1978). Irrespective of which rescaling algorithm is used, if decimal values exist in the range from 0 to 255, they are usually rounded to the nearest integer.

Reflectance Maps Produced on High Resolution Black-and-White CRTs or Film Writers

The Landsat data in an expanded eight-bit format is ideal for display on a high resolution CRT or film writer. Such devices usually have a "bit-map" capability which allows them to fill an individual pixel in the image matrix with any one of 256 shades of gray. Thus, such output devices are ideal for displaying the expanded eight-bit Landsat data because each pixel is assigned a gray scale shade directly proportional to its digital number (DN) value, i.e., the higher the numeric value the lighter the shade assigned to the pixel. No generalization takes place.

An example of film writer output is provided in Figure 1. Note that the resampled 60-m^2 pixels used in this display of an area on the outskirt of Denver, Colorado, take on black, white, and intermediate shades of gray. This is the ideal black-and-white brightness map output medium. Unfortunately, few departments providing remote sensing instruction have access to high resolution CRTs or film writer equipment (Jensen, 1981). The expense of such equipment restricts its availability generally to research organizations in the government and private sectors.

Line Printer Reflectance Maps

The prevalent method of producing a reflectance map is to output a "density-sliced" map to a standard line printer. Density slicing refers to the conversion of the continuous-tone of an image into a series of discrete intervals or slices where each interval corresponds to a specific digital number range (Haralick, 1973). Such slices are analogous to class intervals used in cartography where upper and lower class limits are selected for choropleth, isarithmic, and dasymetric mapping (Robinson *et al.*, 1978).

To produce density sliced maps, it is necessary

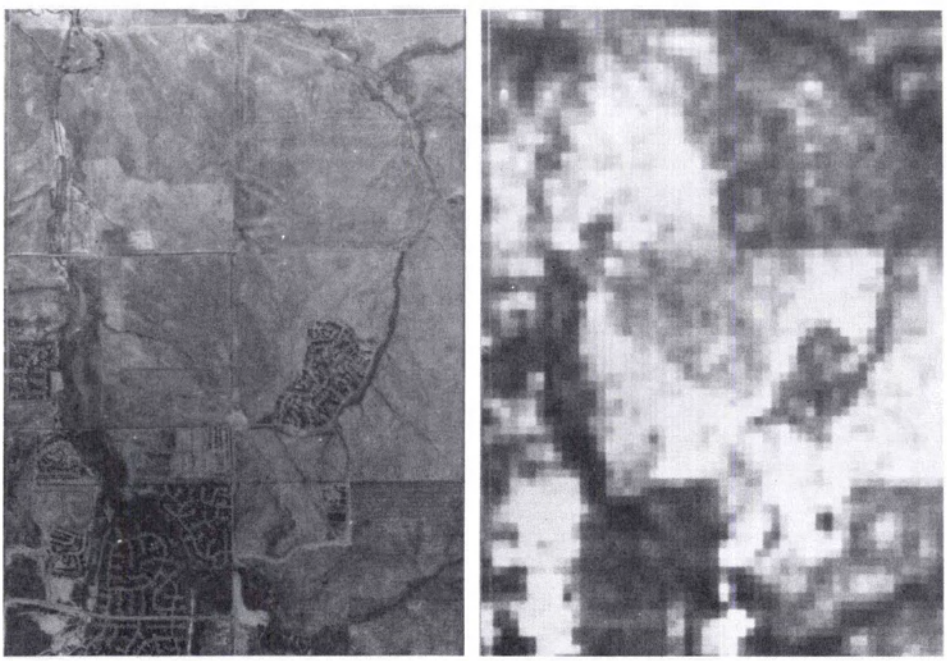

FIG. 1. On the left is a panchromatic aerial photograph of an area near Denver, Colorado, recorded on 8 October 1976. The original scale was 1:52,800. On the right is a 1 October 1976 Landsat MSS band 5 image output on a film writer device with eight-bit resolution. The pixels were resampled to 60-m^2 and a linear contrast stretch was applied to the data.

to select (1) an appropriate number of class intervals, (2) the size or dimension of each class interval, and (3) the symbolization to be assigned to each class interval. Crucial to this task is an awareness of the statistical nature of the scene. The gray level histogram of the Denver, Colorado, Landsat band 5 image is shown in Figure 2. Such histograms summarize the gray level content of the image (Castlemen, 1979). It is a function showing, for each possible digital number (abscissa), the frequency of occurrence of pixels in the image that have that value (ordinate). Analysis of the histogram provides valuable information when selecting the number and dimension of class intervals. One can expect to display successfully about four to eight class intervals on a conventional line printer map (i.e., a two- to three-bit range). Thus, this severely degrades the potential of displaying a truly continuous-tone rendition of the Landsat scene with expanded values ranging from 0 to 255.

There are numerous methods of selecting class interval boundaries, e.g., natural breaks, equal size, equal areas (Jenks and Coulson 1963; MacDougall, 1976). Remote sensing specialists often select the natural break method whereby they analyze the gray scale histogram and then select *n* mutually exclusive class intervals, i.e., density slices, to represent the image. An eight-class density sliced map using natural break criteria is shown in Figure 3a. The equal size and equal area class interval schemes are shown in Figures 3b and 3c, respectively. These algorithms produce a density sliced map with either equal-sized class intervals or approximately equal number of observations in each class interval. Both are ideal for initial evaluations of remotely sensed brightness data.

The paucity of symbols available for creating the impression of continuous tone on a line printer map is also a serious constraint. However, because the line printer is ubiquitous, much research has gone into identifying optimum single print and overprint symbolization to approximate the continuous-tone gray scale (Stucki, 1969; Macleod, 1970; Knowlton and Harmon, 1972; Henderson and Tanimoto, 1974). Recently, improved symbolization for thematic cartography line printer maps was proposed. The results are pertinent to the creation of remote sensing density sliced maps.

Smith (1980) evaluated 47 standard symbols used in computer cartography. Using a transmission densitometer, he measured the "percent area inked" of *areas* of these symbols, which included the empty space between symbols. He then applied the Williams (1958) adjustment to the densitometer values to produce "perceived grayness values" (Table 1). The lightest average gray attainable was 23.2 percent (measured value, not converted) and the darkest was 65.1 percent, giving a range of 41.9 percent. Converted to perceptual equivalence using the Williams curve, the extreme values became 34.5 and 64.1, representing a range of only 29.6 percent (Figure 4). Thus, the ten character per inch and eight line per inch format of the typical line printer caused even the most dense overprint to yield only a 65 percent black area as perceived by the viewer because of the empty space between characters. Such conditions reduce the effectiveness of line printer density sliced maps when used to approximate a continuous-tone image.

When selecting the symbols for each class interval, one should try to develop a graded series which provides adequate contrast between gray

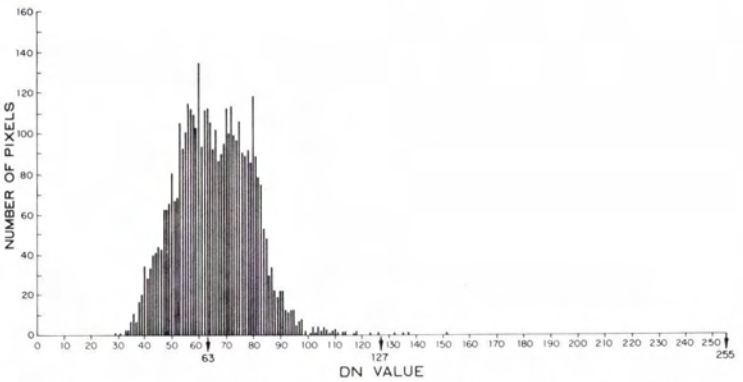

FIG. 2. A histogram of the 1 October 1976 Landsat band 5 subimage displayed in Figure 1. Note that the original Landsat data have been expanded from a seven-bit (0 to 127) to an eight-bit (0 to 255) range. The digital number (DN) values tend to cluster in the lower end of the range, suggesting that it is a rather dark, low contrast scene. The lowest DN value in the subimage is 28 and the highest is 152.

FIG. 3. Density sliced reflectance maps output on a standard eight line per inch line printer. There are eight class intervals in each map. The symbolization is the same in each map and was selected from Table 1 using criteria in Table 2 for eight class interval maps. The first reflectance map's class intervals were selected by examining the histogram in Figure 2 and identifying natural breaks or discontinuities in the data. This is the natural break method. The second map divides the range of the data, i.e., 28 to 152, into eight equal sized class intervals. The final map is based on the selection of eight classes which have approximately the same number of pixels in each class interval. This results in an equal area reflectance map. Line printer reflectance maps such as these with 4 to 16 class intervals are representative of the majority of reflectance maps used in research and education. Note the scale distortion caused by the 4/5 ratio of line to column spacing.

level symbols. Ideally, the contrast is allocated equally between gray-scale symbols. Jenks (1977) suggested that even seven shades of gray in the gray scale progression approached the differentiable limits of the normal map reader. However, his study was based on manuscript, hand-made maps with a tonal range of 100 percent. Therefore, "the limited range of approximately 29 percent transmittance on a line printer map suggests that even five classes" may be too many to display the density sliced map adequately (Smith, 1980).

The eight symbols used in Figure 3 make use of the difference in transmittance information provided in Table 2, i.e., symbols were selected which were approximately 4.22 percent apart. The actual symbol set used is a combination of those suggested by Smith (1980) and MacDougall (1976). The result is useful but points out the obvious limitations of the line printer for producing remote sensing reflectance maps, i.e., that the original data are generalized into a reduced number of class intervals.

Some manufacturers do provide optional gray-scale character sets for line printers (Hamill, 1977; Ballew and Lyon, 1977). Also, some line printers can be adjusted to eradicate the scale distortion (Ballew and Lyon, 1977). But, for the majority of users who only have access to standard eight to six line per inch printers, the creation of brightness maps continues to be a major problem.

Brightness Maps Produced on Plotters

The creation of brightness maps using plotters is another viable alternative. Most educational and research institutions obtain line plotters, electrostatic printer-plotters, and/or dot matrix printer-plotters with dot addressable graphics options. Brightness maps produced by plotters provide (1) greater scaling capability, and (2) the opportunity to create a unique sequence of symbols designed specifically for reflectance maps.

The ability to scale a brightness map accurately so that it overlays a planimetric map base or other image is essential for most serious remote sensing endeavors. For example, the density sliced brightness map in Figure 5 was scaled to overlay precisely the continuous-tone aerial photograph in Figure 1. Scaling is accomplished by calling "scale" subroutines available in the software supplied with most plotters.

TABLE 1. SYMBOLIZATION AND PERCEIVED GRAYNESS BASED ON TRANSMISSION DENSITOMETER MEASUREMENTS†

Symbol	Perceived Grayness (percent)	Symbol	Perceived Grayness (percent)
.	[34.5]	M	46.4
–	25.6	L.	46.4
'	36.4	I–	48.0
+	[38.8]	X–	48.5
/	39.8	/=	48.6
=	[40.5]	X=	50.1
1	40.6	X+	50.5
7	41.5	Z–	50.5
L	41.8	I=	51.6
*	42.0	VT	52.0
I	42.0	O–	[52.9]
5	43.5	VA	53.9
4	43.5	O=	54.4
H	44.0	O/	55.3
3	44.1	O+	55.3
2	44.5	MW	55.9
S	44.8	O*	56.5
X	[44.8]	TVA	57.6
N	44.9	HHH/	58.0
6	45.4	OX	[58.1]
0	45.4	OH=	60.3
9	45.5	MEW	[62.0]*
/–	45.6	OXAV	62.5
8	46.3	HIXO	64.1

† Symbols evaluated in Smith (1980).

* This symbol is suggested in MacDougall (1976). The value is a function of taking a transmission densitometer measurement and converting it to perceived grayness similar to Smith (1980). This value may not be directly comparable to the other values due to differences in printer characteristics.

[ ] Symbols used in Figure 3 were chosen for diagramatic purposes only and should not be considered ideal symbolization for line printer brightness maps.

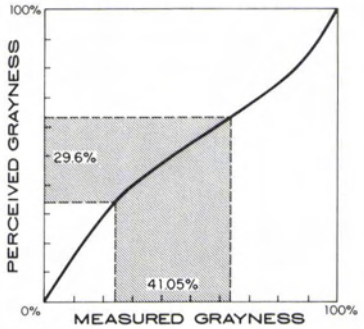

FIG. 4. The range of gray tones produced by overprinting symbols on a line printer is reduced from 41 percent to approximately 30 percent after adjustment according to the Williams curve (after Smith, 1980). The ten character per inch and eight line per inch format typical of line printers causes even the most dense symbolization to yield only a 65 percent black. The blank areas between symbols contributes a great deal to this condition. This graph assumes that the lightest class symbol will not be blank (completely white) because in cartography this is not considered good practice as the map information may be visually confused with the border area surrounding it. However, remote sensing practitioners often use the blank symbol for the highest (brightest) class interval.

Any previously defined alpha-numeric character or symbol in the system software can be called. Often, these are more useful than the standard line printer symbols. In this example, symmetric symbols were chosen to approximate a continuous-tone series. This symbolization is certainly inadequate, and even overprinting of other symbols would only approximate the results produced in the line printer maps.

Other researchers have programmed plotters to turn on specific dots within a pixel (Craig *et al.*, 1978). For example, dot matrix printer-plotter output is shown in Figure 6. Such dot matrices may be used for as many as 16 or even 32 gray levels. However, this procedure still necessitates compressing the data down to a four- or five-bit resolution versus the six- or seven-bit resolution in the raw Landsat data. What is needed are algorithms to produce *any* shade of gray desired (from black to white; 0 to 255, respectively) within each pixel. Such maps hopefully resemble those produced by more expensive film-writer devices. The remainder of this paper addresses this topic.

CROSSED-LINE SHADING

The impression of continuous tone may be produced by using parallel lines, crossed lines, or circular dots located adjacent to one another. This discussion focuses on the use of crossed-line shading for reasons to be discussed. As the name implies, crossed-line shading is produced by intertwining two perpendicular sets of equally spaced parallel lines (Figure 7). The lightness or darkness of the shading is controlled by reducing or increasing the separation between neighboring lines. The width or line thickness (w) is generally held constant while line separation (s) is varied to

TABLE 2. MAXIMUM DIFFERENCE IN GRAY-TONE TRANSMITTANCE FOR A SELECT NUMBER OF CLASS INTERVALS

Number of Class	Line-Printer Map†	Conventional Map
Two	29.6	100
Three	14.8	50
Four	9.93	33.3
Five	7.4	25
Six	5.92	20
Seven	4.93	16.66
Eight	4.22	14.29
Nine	3.7	12.5
Ten	3.29	11.1
Eleven	2.96	10

† Based on the data provided in Table 1 and Figure 4.

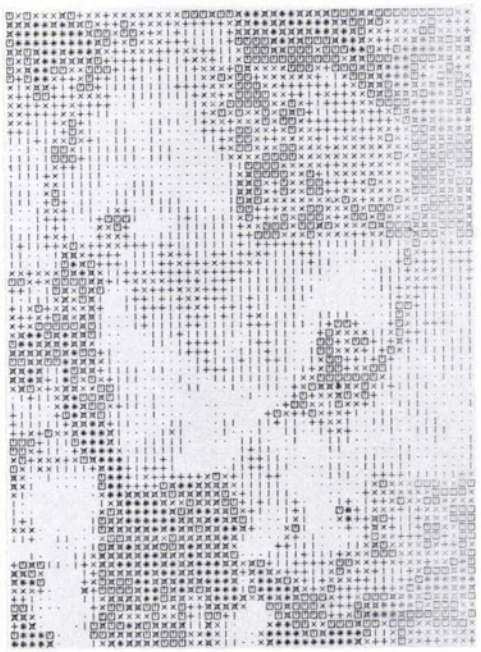

FIG. 5. An eight class reflectance map produced on an electrostatic plotter using symmetric, centered symbols. The output is easily scaled to fit the aerial photography in Figure 1. Unfortunately, the quality of the reflectance map may not be any better than the line printer maps in Figure 3.

produce different tones of gray (Monmonier, 1980).

In order to understand how the proportion of the area inked is computed, consider a typical cell in the shading pattern (Figure 7) as an un-inked square bounded by a half-line-thick frame (Monmonier, 1979). "The inked, or 'black' proportion,

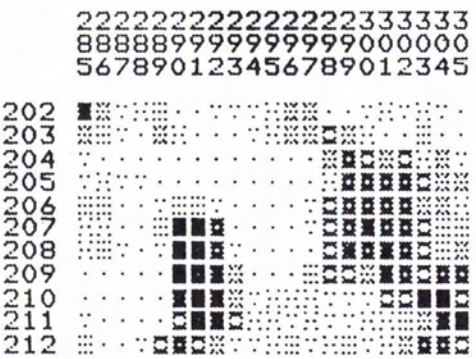

FIG. 6. A portion of brightness map produced on a matrix printer-plotter by turning on specific dots within a pixel. Each of the ten patterns in this example were individually programmed (after Craig *et al.*, 1978). Such results can also be obtained using line plotters or electrostatic printer-plotters.

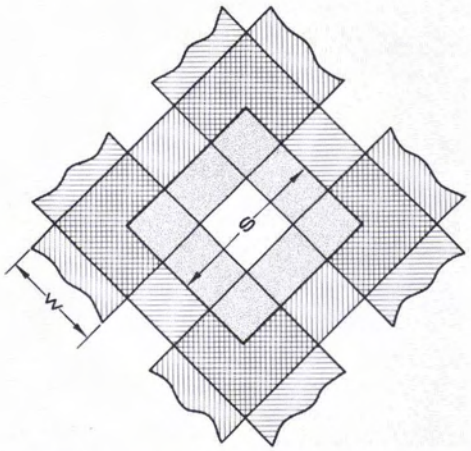

FIG. 7. The geometry of crossed-line shading (after Monmonier, 1980). The line width (w) is generally held constant while line separation (s) is varied using Equation 5 to produce varying shades of gray within a pixel.

p, is the area of this frame, with thickness $w/2$, divided by the total area of the cell formed by lines with separation s, or

$$p = (2s\ (w/2) + 2(s - 2(w/2))\ (w/2))/s^2, \quad (1)$$

which reduces to

$$p = (2sw - w^2)/s^2. \quad (2)$$

Solving this quadratic equation for the plotting separation, s, between neighboring lines yields

$$s = (w + w(1 - p)^{1/2})/p." \quad (3)$$

In the original work by Tobler (1973) on crossed-line continuous-tone mapping, the proportion, p, was rescaled according to the psychophysical power function

$$R = S^{1/a} \quad (4)$$

which relates response of the map reader, R, to map stimulus, S. "In the rescaled formula

$$s = (w/p^a)\ (1 + (1 - p^a)^{1/2}) \quad (5)$$

where p now represents the intended proportion rather than the apparent proportion of the area inked" (Monmonier, 1979).

Based on work by Stoessel (1972), "Tobler derived a correction for continuous-tone crossed-line shading with the exponential function Area Inked = Value$^{1.4}$, which represents the perceptual transformation Value = (Area Inked)$^{0.7}$" (Monmonier, 1980). This transformation is labeled Exponential-Stoessel (Tobler) in Figure 8. Thus, when the exponent a is set to 1.4, the non-linear response of the human perceptual system is taken into consideration. Other exponents have been proposed such as, Value = (Area Inked)$^{0.645}$ which, obviously, produces similar results (Peterson, 1979).

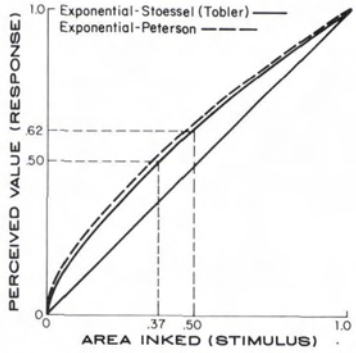

FIG. 8. Two models which compensate for the nonlinear response of the human eye to percent area inked stimuli.

To use Equation 5, the Landsat pixel value, p_i, must be transformed into value p, which lies within the range from 0 to 1. Each pixel value, p_i, is recomputed according to the formula

$$p = (p_i - R_{min})/(R_{max} - R_{min}) \qquad (6)$$

where R_{min} and R_{max} represent the extreme points in the total range of values which p_i might take upon itself, e.g., 0 to 255.

CONTRAST ENHANCEMENT

If Landsat pixel values for a given scene are not uniformly distributed throughout the entire 0 to 255 range, as exemplified by the histogram in Figure 2, the application of Equation 5 produces a continuous-tone map with very little contrast (Figure 9a). Landsat scenes are often low in contrast (Hummel, 1977). Consequently, it is often necessary to apply some type of contrast enhancement so that the dynamic range of the output device is used to maximum potential, i.e., there exists a clear representation of blacks, whites, and grays on the final reflectance map.

There are numerous contrast stretch algorithms which may be employed (Sabins, 1978; Castleman, 1979). One of the more widely used is the simple linear contrast stretch (Soha *et al.*, 1976; Harris, 1977; McKinney, 1978). Such a stretch can be generated by mapping each digital number (DN) value encountered in the image, pixel by pixel, to the range 0 to 255 by the linear equation

$$p_i = ((p_i' - H_{min})/(H_{max} - H_{min}))\ 255 \qquad (7)$$

where p_i' is the raw DN value and p_i is the new DN value after it has been stretched. H_{min} and H_{max} are the minimum and maximum values of the histogram range which the user specifies after evaluating the shape and dimension of the histogram. For example, the lower DN value in the histogram shown in Figure 2 is 28 with the highest being 152. If these values are used as H_{min} and H_{max} values in Equation 7, the result is shown in Figure 9b. Note that some improvement in contrast is apparent. To enhance the contrast, it is useful to select H_{min} and H_{max} values some percentage in from the extreme values. For example, Figures 9c and 9d depict contrast stretches of 2 and 4 percent. In figure 9d, the lower 4 percent of the pixels (i.e., DN < 40 are assigned to black, or 0, and the upper four percent DN > 93) are assigned to white, or 255. The remaining pixel values are distributed linearly between these extremes. This results in a brightness map with good contrast and one which approximates the quality of the film writer output in Figure 1. Of course, the matrix of contrast stretched pixel values must be scaled to lie between 0 and 1, using Equation 6 before input to Equation 5.

Experience has shown that the use of these equations will produce excellent crossed-line shading brightness maps using either line plotters or electrostatic printer-plotters. Electrostatic plotters have the significant advantage, however, of not requiring thousands of pen movements when drawing the vectors. Consequently, brightness maps are produced more rapidly using the electrostatic plotter.

REPRODUCTION CONSIDERATIONS

The use of a perceptual exponent, a, and contrast stretched data do not guarantee that the crossed-line methodology will result in a useful brightness map. Another critical element is "edge-growth," which can take place as the plotter output map is photographed, then duplicated for reproduction (Monmonier, 1979). This means that the crossed lines begin to 'bleed' into one another as the map is reproduced. The graphs in Figure 10 demonstrate the edge-growth (g) which may be expected for line widths of 0.1 mm and 0.5 mm, assuming an edge or line growth of 0.1 mm or 0.025 mm. The top two illustrations simulate the effects of edge-growth on parallel-line shading while the bottom pair simulates the effects of edge-growth on cross-line shading discussed in this paper. Analysis of the graphs reveals that crossed-line shading is the more graphically stable area symbol method. It maintains more stability, especially toward the upper end of the data range. If the effects of edge-growth are not taken into consideration, the impact can overwhelm the use of the perceptual scaling exponent, a. The user must experiment to find optimum line width (w), spacing (s), and degree of edge growth (g) allowable for a given plotter and subsequent reproduction system.

CONCLUSIONS

Algorithms for the production of continuous-tone brightness maps on an electrostatic plotter

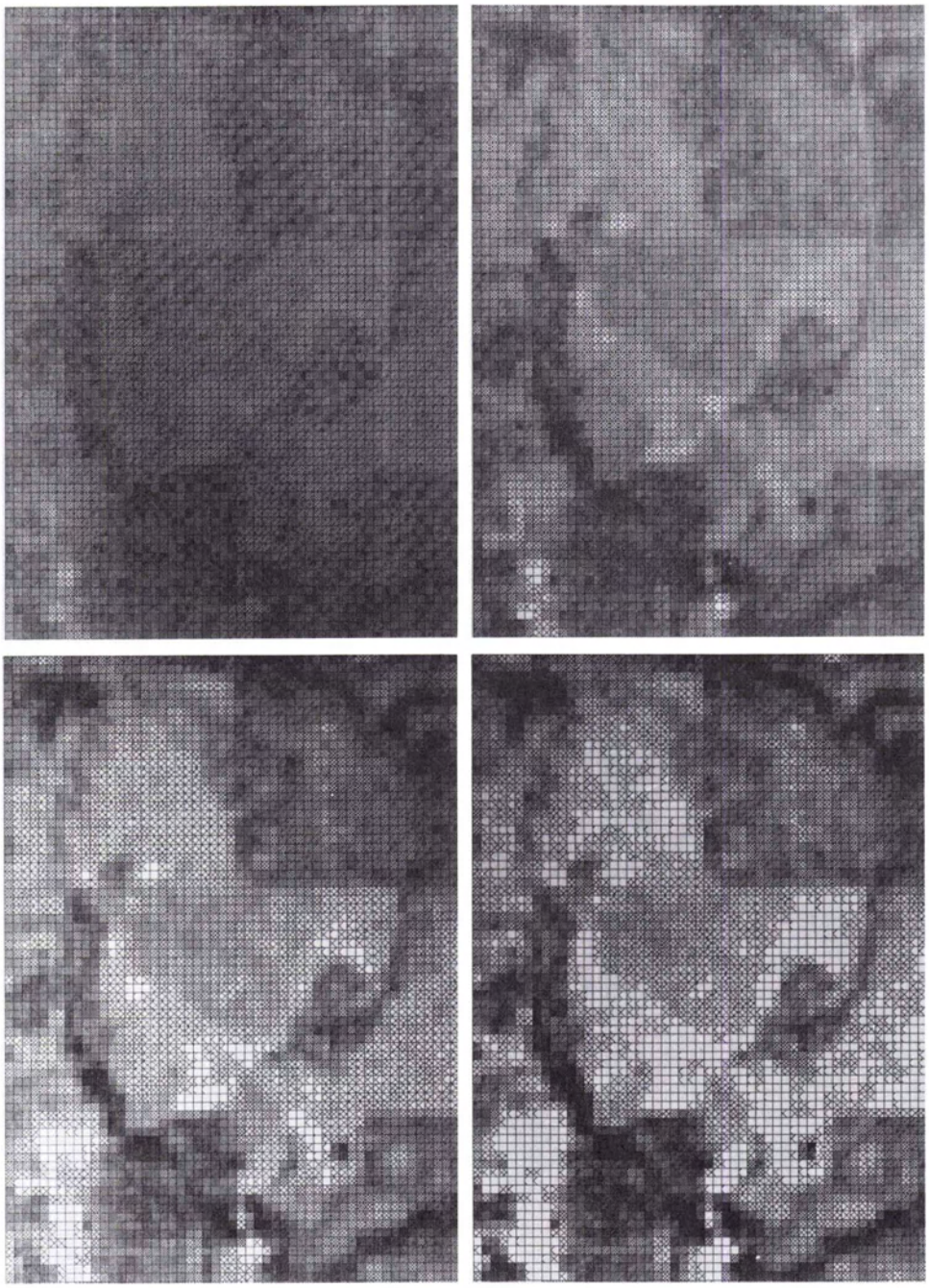

FIG. 9. Remote sensing reflectance maps produced by the cross-line Equation 5. Figure 9a (top left) displays the results of applying Equation 5 to the low contrast Landsat data. The results is a very low contrast image. Figure 9b is a reflectance map of the same area but with a linear contrast stretch applied with the minimum and maximum set to 28 and 152, i.e., the extremes of the data range found in the histogram (Figure 2). Figures 9c and 9d represent linear contrast stretches of 2 and 4 percent applied to the data before input to Equation 5. Note that the contrast improves dramatically. The pixel size was 0.14 inch square with a line width (w) of 0.02 inch. The spatial resolution of the electrostatic printer-plotter used was 200 dots per inch (0.005 inch). The original brightness maps were reduced photographically by 60 percent.

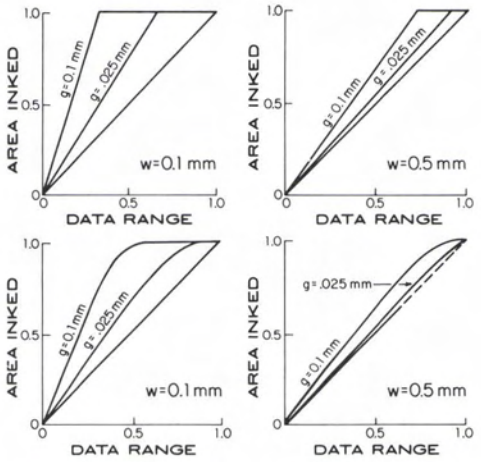

FIG. 10. Simulated effects of photographic reproduction edge-growth on parallel-line and crossed-line shading. The upper two graphs show expected edge growth (g) using parallel-line symbolization and 0.1-mm and 0.5-mm line widths (w). The lower graphs display the same information for crossed-line shading. "In contrast to parallel-line shading, the crossed-line curves have a definite warp, which is more pronounced for greater amounts of edge growth. Parallel-line shading, with neighboring lines steadily approaching each other as the intended proportion of black increases, is abruptly filled-in by edge growth, whereas crossed-line patterns, with neighboring shading lines advancing less rapidly toward the centers of the shrinking, uninked interstices, are not so readily obscured by fill-in" (Monmonier, 1980). This is one reason that the crossed-line method is superior for remote sensing reflectance maps.

have been reviewed. The brightness maps produced using cross-lined symbolization may be improved by

- selecting an appropriate perceptual scaling exponent,
- applying a practical contrast enhancement algorithm to the raw data, and
- being aware that edge-growth will occur and plan accordingly by not selecting too wide (w) a line width or too close a line space (s) in view of the reproduction which will take place.

Experimentation with the algorithms and awareness of the output device idyosyncracies will enable remote sensing brightness maps to be produced economically which rival those produced on more expensive output devices.

REFERENCES

Ballew, G. I., and R. J. P. Lyon, 1977. The Display of Landsat Data at Large Scales by Matrix Printer, *Photogrammetric Engineering and Remote Sensing*, Vol. 43, No. 9, pp. 1147-1150.

Benson, Perry, and Mortimer L. Mendelsohn, 1964. Picture Generation with a Standard Line Printer, *Communications of the ACM*, Vol. 7, No. 5, pp. 311-314.

Brassel, Kurt, 1974. A Model for Automated Hill Shading, *The American Cartographer*, Vol. 1, No. 1, pp. 15-27.

Carter, Virginia, Frederick Billingsley, and Jeannine Lamar, 1977. *Summary Tables for Selected Digital Image Processing Systems*, Open-File Report 77-414, U.S. Geological Survey, 45 pages.

Castlemen, Kenneth R., 1979. *Digital Image Processing*, New Jersey: Prentice-Hall, pp. 68-95.

Coppock, J. R., 1975. Maps by Line Printer, in John C. Davis and Michael J. McCullagh (Eds) *Display and Analysis of Spatial Data*, John Wiley & Sons, New York, 146 p.

Craig, Michael E., Richard Sigman, and Manuel Cardenas, 1978. *Area Estimates by Landsat: Kansas 1976 Winter Wheat*, Report of the New Techniques Section of the Economics, Statistics, and Cooperative Service of the U.S. Department of Agriculture. Washington, D.C., 12 p.

Hamill, Philip, 1977. Line Printer Modification for Better Gray Level Pictures, *Computer Graphics and Image Processing*, Vol. 6, pp. 485-491.

Haralick, Robert M., 1973. Glossary and Index to Remotely Sensed Image Pattern Recognition Concepts, *Pattern Recognition*, Vol. 5, pp. 391-403.

Harris, George, 1977. A Low Throughput Digital Image Enchancement System, *Proceedings, International Symposium on Image Processing*, Interactions with Photogrammetry and Remote Sensing, Graz, Germany, pp. 79-87.

Henderson, Peter, and Steven Tanimoto, 1974. Considerations for Efficient Picture Output via Line Printer, *Computer Graphics and Image Processing*, Vol. 3, pp. 327-335.

Horn, Berthold K. P., 1981. Hill Shading and the Reflectance Map, *Proceedings of the IEEE*, Vol. 69, No. 1, pp. 14-47.

Horn, Berthold K. P., and Robert W. Sjoberg, 1979. Calculating the Reflectance Map, *Applied Optics*, Vol. 18, No. 11, pp. 1770-1779.

Hummel, Robert, 1977. Image Enhancement by Histogram Transformation, *Computer Graphics and Image Processing*, Vol. 6, pp. 184-195.

Jenks, George F., 1977. *Optimal Data Classification for Choropleth Maps*, Occasional Paper No. 3, Department of Geography, The University of Kansas, Lawrence.

Jenks, George F., and Michael R. C. Coulson, 1963. Class Intervals for Statistical Maps, *International Yearbook of Cartography*, Vol. 3, pp. 119-133.

Jensen, John R., 1981. Educational Image Processing: An Overview, *Proceedings, ASP Fall Technical Meeting*, San Francisco, pp. 142-155.

Jensen, John R., Fred A. Ennerson, and Earl J. Hajic, 1979. An Interactive Image Processing System for Remote Sensing Education, *Photogrammetric Engineering and Remote Sensing*, Vol. 45, No. 11, pp. 1519-1527.

Knowlton, Ken, and Leon Harmon, 1972. Computer-Produced Grey Scales, *Computer Graphics and Image Processing*, Vol. 1, No. 1, pp. 1-20.

Macleod, I. D. G., 1970. Pictorial Output with a Line Printer, *IEEE Transactions on Computers*, pp. 160-162.

MacDougall, E. Bruce, 1976. *Computer Programming for Spatial Problems*, London: Edward Arnold, 160 pages.

McKinney, R. L., 1978. *Comparison of Large Scene Image Enhancement Capabilities at GSFC*, Report NAS 5-24350 #206, Computer Sciences Corporation for Goddard Space Flight Center, Greenbelt, Maryland, 25 pages.

Monmonier, Mark S., 1979. Modelling the Effect of Reproduction Noise on Continuous-tone Area Symbols, *The Cartographic Journal*, Vol. 16, No. 2, pp. 86-96.

———, 1980. The Hopeless Pursuit of Purification in Cartographic Communication: A Comparison of Graphic Arts and Perceptual Distortions of Graytone Symbols, *Cartographica*, Vol. 17, No. 1, pp. 24-39.

Peterson, Michael P., 1979. An Evaluation of Unclassed Crossed-Line Choropleth Mapping, *The American Cartographer*, Vol. 6, No. 1, pp. 21-37.

Robinson, Arthur H., Randall Sale, and Joel Morrison, 1978. *Elements of Cartography*, New York: John Wiley and Sons, 266 pages.

Sabins, Floyd R., 1978. *Remote Sensing Principles and Interpretation*, San Francisco: W. H. Freeman, pp. 248-254.

Smith, Richard M., 1980. Improved Areal Symbols for Computer Line-Printer Maps, *The American Cartographer*, Vol. 7, No. 1, pp. 51-58.

Soha, J. M., A. R. Gillespie, M. J. Abrams, and D. P. Madura, 1976. Computer Techniques for Geological Applications, *Proceedings, Caltech/JPL Conference on Image Processing Technology*. Jet Propulsion Lab SP 43-30, pp. 4.1 to 4.21.

Stoessel, Otto C., 1972. Standard Color Screen Tint Systems for Department of Defense Mapping, Charting and Geodesy Services, Part II: Standard Printing Screen System, *Proceedings, ACSM Fall Technical Meeting*, pp. 111-149.

Stucki, P., 1969. Generation of Grey Tones by Computer for Simulation of Visual Information Systems, *IEEE Transactions on Computers*, pp. 642-643.

Tobler, Waldo R., 1973. Choropleth Maps Without Class Intervals? *Geographical Analysis*, Vol. 5, No. 3, pp. 262-265.

Yoeli, Pinhas, 1966. Analytical Hill Shading and Density, *Surveying and Mapping*, Vol. 26, No. 2, pp. 253-259.

(Received 13 August 1981; revised and accepted 30 June 1982)

CALL FOR PAPERS

International Colloquium on Spectral Signatures of Objects in Remote Sensing

Bordeaux, France
13-16 September 1983

The Colloquium is being organized by the Institut National de la Recherche Agronomique (I.N.R.A.) and is supported by the International Society for Photogrammetry and Remote Sensing (Commission VII, Working Group 3) and the Centre National d'Etudes Spatiales (C.N.E.S.). It will include sessions on

- Spectral characterization of optimal spectral bands, equipments, and methods.
- Influence of measurement conditions on obtained radiometric signal (climatic factors, sun position, view angle, etc.).
- Influence of the surface state on the radiometric response of objects (roughness, geometry of the vegetative canopy, state of the water).
- Problems set by the transposition to aerospatial measurements of ground level radiometric data.
- Studies that precede the use of spectral bands of intending spatial systems.

Those wishing to present papers should submit a 200 to 300 word abstract in French or English before *15 March 1983* to

J. Riom
I.N.R.A.
Laboratoire de Télédétection Pierroton
Pierroton 33610 Cestas, France